Acta Cryst. (1998). D**54**, 659–661

Crystallization and preliminary X-ray diffraction analysis of aspartate aminotransferase from *Saccharomyces cerevisiae*

CONSTANCE J. JEFFERY,[a] TOM BARRY,[b] SHAWN DOONAN,[b]† GREGORY A. PETSKO[a] AND DAGMAR RINGE[a]* *at* [a]*Rosenstiel Basic Medical Sciences Research Center, Brandeis University, Waltham, MA 02254, USA, and* [b]*Department of Biochemistry, University College Cork, Lee Maltings, Prospect Row, Cork, Ireland. E-mail: ringe@binah.cc.brandeis.edu*

(*Received 19 August 1997; accepted 10 November 1997*)

Abstract

Diffraction-quality crystals of *S. cerevisiae* cytoplasmic aspartate aminotransferase have been obtained by the hanging-drop vapor-diffusion method in the presence of pyridoxal phosphate and maleic acid, sodium acetate, ammonium acetate and polyethylene glycol. The crystals have the symmetry of the orthorhombic space groups $P2_12_12_1$ or $P2_12_12$ with unit-cell dimensions a = 130.2, b = 134.6 and c = 98.7 Å. Square rod-shaped crystals with dimensions of approximately 0.2 × 0.2 × 0.5 mm diffract to spacings of 2 Å. The calculated value of the Matthews coefficient, V_m = 2.4 Å^3 Da^{-1}, is consistent with four subunits of aspartate aminotransferase per asymmetric unit.

1. Introduction

Pyrodoxal phosphate (PLP) serves as a cofactor in many enzymatic reactions that involve amino-acid transamination, racemization, decarboxylation or isomerization. In order to elucidate the role of the PLP cofactor in these reactions, crystal structures have been determined for several PLP-dependent enzymes. Aspartate aminotransferase (L-Asp-AT) catalyzes the reversible reaction

L-aspartate + 2-oxoglutarate ⟷ oxaloacetate + L-glutamate.

A detailed understanding of the complex reaction mechanism, catalytic residues, and role of the PLP cofactor in this enzyme has been greatly aided by comparison of the structure and function of aspartate aminotransferases from several organisms. Crystal structures are available for L-Asp-AT from *E. coli* (Smith *et al.*, 1989; Okamoto *et al.*, 1994; Jager *et al.*, 1994), chicken cytoplasm and mitochondria (Ford *et al.*, 1980; McPhalen *et al.*, 1992; Borisov *et al.*, 1985; Harutyunyan *et al.*, 1985; Malashkevich *et al.*, 1995) and pig cytoplasm (Arnone *et al.*, 1985). These proteins share a similar three-dimensional fold although they share only about 40% amino-acid sequence identity (except for the two cytosolic isozymes, which share 83% sequence identity). A comparison of these structures to the L-Asp-AT structure from a unicellular eukaryote would provide more details about the catalytic mechanism and evolution of this family of proteins. In addition, this comparison would add to our understanding of how different sequences can fold into similar structures. The cytosolic isozyme from the yeast *Saccharomyces cerevisiae* shares less than 50% amino-acid identity with any of the aspartate aminotransferases for which structures are available (Cronin *et al.*, 1991). We have undertaken to obtain a high-resolution structure of the *S. cerevisiae* cytoplasmic aspartate aminotransferase in the presence of maleic acid. Maleic acid is a competitive inhibitor of the enzyme that mimics the structure of the substrate, and thereby provides information about the binding and interactions of the substrate with the protein. In addition, this inhibitor induces the conformational change that the enzyme is known to undergo upon binding substrate. We report here the crystallization and preliminary X-ray characterization of *S. cerivisiae* cytoplasmic aspartate aminotransferase.

2. Methods

S. cerivisiae cytoplasmic aspartate aminotransferase was prepared from wild-type yeast cells as described previously (Cronin *et al.*, 1991) and appeared as a single band on a Coomassie-stained sodium dodecyl sulfate (SDS) polyacrylamide gel. The protein was dialyzed against buffer containing 10 μ*M* PLP. After concentration, maleic acid was added so that the final protein solution contained 5–15 mg ml^{-1} aspartate aminotransferase, 10 m*M* sodium acetate, pH 5.8, 10 μ*M* PLP, and 100 μ*M* maleate. The final protein concentration was determined by the method of Bradford (1976).

Sparse-matrix crystal screening was carried out based on the method of Jancarik & Kim (1991). Several conditions employing PEG or MPD as the precipitant yielded yellow

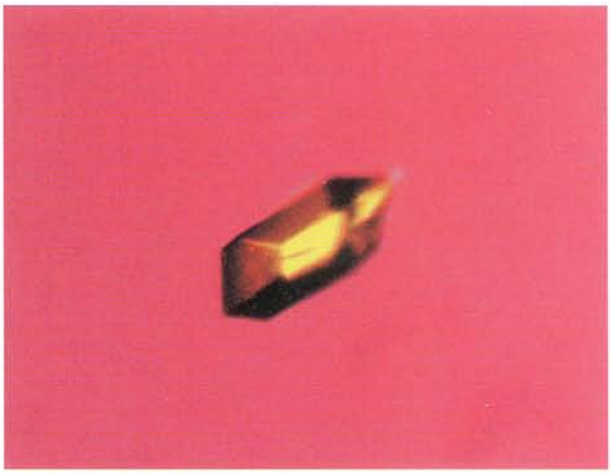

Fig. 1. Crystal of *S. cerevisiae* cytoplasmic aspartate aminotransferase. The approximate dimensions of this crystal are 0.2 × 0.2 × 0.5 mm.

† Current address: Department of Life Sciences, University of East London, Romford Road, Stratford, London E15 4LZ, England.

crystals that were very small rods or thin plates. Crystal size and morphology were improved by modifying the protein concentration, the concentration and molecular weight of PEG, macroseeding, microseeding, varying the ratio of protein solution to reservoir solution, and by using different buffers and acetate salts. The best crystals were obtained at room temperature by the hanging-drop method of vapour diffusion in 24-well Linbro dishes with siliconized cover slips. Hanging drops contained 2 µl of protein solution and 4 µl of well solution and were allowed to equilibrate against 1 ml of well solution. Crystals appeared 1–5 d after setting up the drops, but the best single crystals were obtained by microseeding drops in which no crystals appeared after the first 2 d. The final crystallization drops contained 5–15 mg ml^{-1} aspartate aminotransferase, 10 µ*M* PMSF, 10 µ*M* PLP, 10 m*M* sodium acetate buffer, pH 5.8, and 100 µ*M* sodium maleate in the protein solution and 0.2 *M* ammonium acetate, 0.1 *M* acetate buffer, pH 4.6, and 22–20% PEG 4000 in the reservoir solution. Some crystals grew to 0.2 × 0.2 × 0.7 mm in size.

Single crystals were mounted in thin-walled quartz capillary tubes and X-ray diffraction data were collected at 277 K with a 0.3 mm collimator on an R-Axis IIC imaging-plate system, using Cu *K*α radiation (λ = 1.54 Å) from a Rigaku RU200-HB rotating-anode generator operating at 50 kV and 145 mA. The crystal-to-detector distance was 100 mm. Crystals were kept at a temperature of 277 K with a stream of chilled air.

Still photos were used in indexing to determine unit-cell parameters. A native data set was obtained with an oscillation range of 1° for a total of 47° with a 30 min exposure per frame. The data frames were integrated, scaled, and merged with standard R-Axis software (Wonacott, 1980; Higashi, 1990).

A self-rotation function was calculated using the program *GLRF* (Tong & Rossman, 1990, 1997). Patterson map *A* was calculated with 11 917 reflections between 10.0 and 4.0 Å resolution. The large-term cutoff was 1.5, so that 2 603 reflections were used in the calculation of Patterson map *B*. The radius of integration was 20 Å.

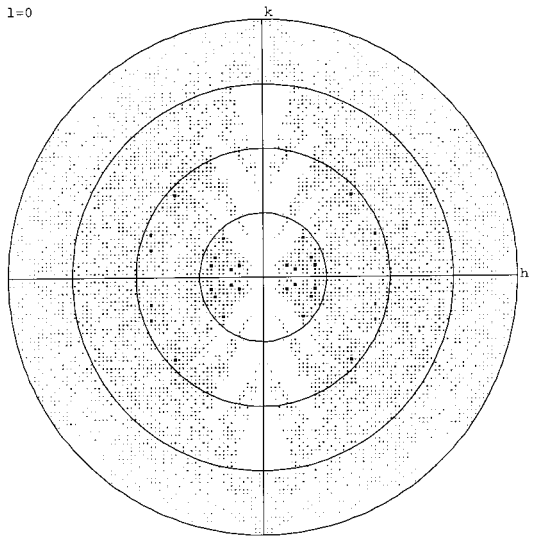

Fig. 2. A pseudoprecession plot of the *hk*0 zone calculated using the program *HKLVIEW* from the *CCP*4 suite (Collaborative Computational Project, Number 4, 1994). The outer circle of the pattern shows 2.0 Å resolution.

3. Results and discussion

Single crystals of approximately 0.2 × 0.2 × 0.5 mm diffracted to 2.0 Å spacings. The best diffracting crystals had a square rod morphology and bright yellow color like that shown in Fig. 1. The crystals were moderately sensitive to X-ray decay but last over 48 h in the X-ray beam at 277 K. Indexing of three frames gave unit-cell parameters of a = 130.2, b = 134.6 and c = 98.7 Å. The symmetry of the diffraction pattern in the still photos was consistent with a primitive orthorhombic space group.

A complete native data set was obtained by measuring intensities for 470 081 reflections, with an R_{sym} of 12% on intensities. The final merged data set contained 101 176 reflections with $I/\sigma(I) > 0$, corresponding to 93% completeness in the resolution range of 15–2.0 Å (85% in the resolution range from 2.3–2.0 Å). A graphical representation of the *hk*0 zone of the data is shown in Fig. 2.

The final merged data set was used to determine the actual space group to which the data belong. Systematic absences in the diffraction pattern are consistent with a space group of $P2_12_12$ or $P2_12_12_1$. The calculated molecular weight of the protein is 45.3 kDa per subunit; assuming four monomers per asymmetric unit yields a Matthews coefficient of 2.4 Å^3 Da^{-1} (Matthews, 1968) with a solvent content of 49%. Analysis of a self-rotation function of the data (Fig. 3) indicates that there are multiple twofold axes of symmetry, but that there is not a fourfold axis of symmetry. This is consistent with there being two dimers in the asymmetric unit. We are currently using the molecular-replacement method to solve the structure.

This work was supported by a Cystic Fibrosis Foundation Postdoctoral Fellowship to CJJ and NSF Grant No. MCB9317373.

References

Arnone, A., Rogers, P. H., Hyde, C. C., Briley, P. D., Metzler, C. M. & Metzler, D. E. (1985). *Transaminases*, edited by P. Christen & D. E. Metzler, pp. 138–155. New York: John Wiley & Sons.

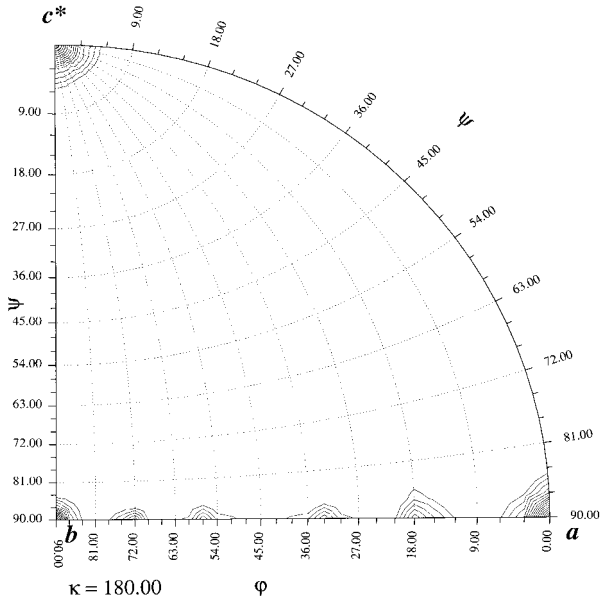

Fig. 3. A plot of the self-rotation function calculated using the program *GLRF* (Tong & Rossman, 1990, 1997).

Borisov, V. V., Vorizova, S. N., Kachalova, G. S., Sosfenov, N. I. & Vainstein, B. K. (1985). *Transaminases*, edited by P. Christen & D. E. Metzler, pp. 155–164. New York: John Wiley & Sons.
Bradford, M. M. (1976). *Anal. Biochem.* **72**, 248–254.
Collaborative Computational Project, Number 4. (1994). *Acta Cryst.* D**50**, 760–763.
Cronin, V. B., Maras, B., Barra, D. & Doonan, S. (1991). *Biochem. J.* **277**, 335–340.
Ford, G. C., Eichele, G. & Jansonius, J. N. (1980). *Proc. Natl Acad. Sci. USA*, **77**, 2559–2563.
Harutyunyan, E. G., Malashkevich, V. N., Kochkina, V. M. & Torchinsky, Y. M. (1985). *Transaminases*, edited by P. Christen & D. E. Metzler, pp. 164–173. New York: John Wiley & Sons.
Higashi, T. (1990). *Process: A Program for Indexing and Processing R-AXIS IIC Imaging Plate Data*, Rigaku Corporation, Danvers, MA, USA.
Jager, J., Moser, M., Sauder, U. & Jansonius, J. N. (1994). *J. Mol. Biol.* **239**, 285–305.
Jancarik, J. & Kim, S.-H. (1991). *J. Appl. Cryst.* **24**, 409–411.
McPhalen, C., Vincent, M. G. & Jansonius, J. N. (1992). *J. Mol. Biol.* **225**, 495–517.
Malashkevich, V. N., Strokopytov, B. V., Borisov, V. V., Dauter, Z., Wilson, K. S. & Torchinsky, Y. M. (1995). *J. Mol. Biol.* **247**, 111–124.
Matthews, B. W. (1968). *J. Mol. Biol.* **33**, 491–497.
Okamoto, A., Higuchi, T., Hirotsu, K., Kuramitsu, S. & Kagamiyama, H. (1994). *J. Biochem. (Tokyo)*, **116**, 95–107.
Smith, D. L., Almo, S. C., Toney, M. D. & Ringe, D. (1989). *Biochemistry*, **28**, 8161–8167.
Tong, L. & Rossman, M. G. (1990). *Acta Cryst.* A**46**, 783–792.
Tong, L. & Rossman, M. G. (1997). *Methods Enzmol.* **276**, 594–611.
Wonacott, A. J. (1980). *MOSFLM: A Suite of Programs for On-line Evaluation and Analysis of Integrated Intensities on Small Angle Rotation/Oscillation Photographs*, Imperial College, London, England.